Strings Attached – Oligothiophene Substituents Determine the Fate of Excited States in Ruthenium Complexes for Photodynamic Therapy

Avinash Chettri[1,2], Kilian R. A. Schneider[1,2], Houston D. Cole,[3] John A. Roque III,[3,4] Colin G. Cameron,[3] Sherri A. McFarland[3], Benjamin Dietzek[1,2*]*

[1]Leibniz-Institute of Photonic Technology Jena, Department Functional Interfaces, Albert-Einstein-Straße 9, 07745 Jena, Germany

[2]Friedrich-Schiller University Jena, Institute of Physical Chemistry and Abbe Center of Photonics, Helmholtzweg 4, 07743 Jena, Germany

[3]The University of Texas at Arlington, Department of Chemistry and Biochemistry, Arlington, TX 76019, USA

[4]The University of North Carolina at Greensboro, Department of Chemistry and Biochemistry, Greensboro, NC 27402, USA

*Corresponding authors: sherri.mcfarland@uta.edu and benjamin.dietzek@leibniz-ipht.de

Keywords: TLD1433; photodynamic therapy; excited-state relaxation; long-lived triplet states

ABSTRACT

We explore the photophysical properties of a family of Ru(II) complexes, **Ru-ip-*n*T**, designed as photosensitizers for photodynamic therapy (PDT). The complexes incorporate a 1*H*-imidazo[4,5-*f*][1,10]-phenanthroline (ip) ligand appended to one or more thiophene rings. One of the complexes studied herein, **Ru-ip-3T** (known as TLD1433), is currently in Phase II human clinical trials for treating bladder cancer by photodynamic therapy (PDT). The potent photocytotoxicity of **Ru-ip-3T** is attributed to a long-lived intraligand charge-transfer triplet state. The accessibility of this state changes upon varying the length (*n*) of the oligothiophene substituent. In this paper we highlight the impact of *n* on the ultrafast photoinduced dynamics in **Ru-ip-*n*T**, leading to the formation of the function-determining long-lived state. Femtosecond time-resolved transient absorption combined with resonance Raman data was used to map the excited-state relaxation processes from the Franck-Condon point of absorption to the formation of the lowest-energy triplet excited state, which is a triplet metal-to-ligand charge transfer (^{3}MLCT) excited state for **Ru-ip-0T**-**1T** and an oligothienyl-localized triplet intraligand charge transfer (^{3}ILCT) excited state for **Ru-ip-2T**-**4T**. We establish the structure-activity relationships with regard to changes in the excited state dynamics as a function of thiophene chain length, which alters the photophysics of the complexes and presumably impacts the photocytotoxicity of these photosensitizers.

INTRODUCTION

Photodynamic therapy (PDT) involves the use of light to activate an otherwise nontoxic photosensitizer (PS) to target cancer cells or pathogens.[1–3] An advantage of PDT is that toxicity is confined to regions where the PS, light and oxygen overlap spatiotemporally. The primary mechanism of PDT is the generation of cytotoxic singlet oxygen by the PS through Type II energy transfer, but other reactive oxygen species (ROS) formed via Type I electron transfer processes can contribute. Currently, there are only a handful of PSs approved for PDT, and these are largely porphyrin-derived.

Photoactive transition metal complexes for PDT constitute an emerging class of PSs.[4–6] Combining different metals with various ligands controls the absorption characteristics of the complexes to shift light-absorption to the relevant spectral region for a given application.[7,8] The choice of ligands also modulates cellular uptake and distribution of the complexes in the cells and tunes the nature of the lowest-energy excited states and their intrinsic lifetimes, which appear to be key to their action as PDT agents.[9,10] Certain metal complexes bearing π-expansive ligands appended to organic chromophores have prolonged triplet state lifetimes (tens of microseconds or longer).[10–17] Such long lived triplet excited states are characteristic of organic chromophores, but their quantum yield for triplet state formation is generally quite limited in organic systems.[18–20] Tethering π-expanded organic chromophores to photoactive transition metal complexes has proven to be an effective strategy for capitalizing on the high spin orbit coupling (SOC) afforded by the metal center for more efficient triplet state formation.[21,22] This is possible in metal-organic dyads that have low-energy ligand-localized excited states in close proximity to the lowest lying triplet metal-to-ligand charge transfer (^{3}MLCT) excited states that generally dominate the photophysics of Ru(II) polypyridyl complexes.[14] Population of these triplet intraligand (^{3}IL) excited states from the initially formed ^{1}MLCT or ^{1}IL states can yield ^{3}IL states with intrinsic lifetimes exceeding 50 μs.[11] These long-lived triplet states interact efficiently with $^3O_2$[23] rendering such complexes potent candidates for PDT.[14]

The McFarland group introduced the Ru(II) complex TLD1433 (**Ru-ip-3T**, $[Ru(4,4'\text{-dmb})_2(IP\text{-}3T)]Cl_2$ where 4,4′-dmb=4,4′-dimethyl-2,2′-bipyridine and ip-3T=2-(2′,2″:5″,2‴′-terthiophene)-imidazo[4,5-*f*][1,10]phenanthroline) as a PS for PDT, which is currently in Phase II human clinical trials for treating non-muscle invasive bladder cancer (ClinicalTrials.gov Identifier: NCT03945162).[18–20] The photosensitizing capacity of TLD1433 is associated with long lived, low lying triplet ligand-centered states involving the α-terthiophene chain (*n*T). The α-terthiophene is key to the potent generation of singlet oxygen,[7,18,24–27] but other mechanisms could be at play, especially given that the ligand-localized triplet for TLD1433 is predominantly intraligand charge transfer (ILCT) in character and oligothiophenes in general can form charge-separated species.[28]

This work interrogates the ultrafast dynamics of TLD1433 and related compounds that differ systematically in the number of thiophene rings (from 1T to 4T, Figure 1a). We highlight the primary photoinduced processes leading to the population of the photobiologically relevant long-lived triplet states that were detailed in a previous study, where it was shown that the singlet oxygen quantum yields increase (and emission quantum yields decrease) with the length of the thiophene chain.[29] Here, we explore the **Ru-ip-*n*T** (*n*=0-4) series and show the impact of the initial excitation wavelength on the excited-state relaxation pathway and the population of the long-lived excited states.[29]

METHODS

Samples. All experiments were performed on the chloride salts of the **Ru-ip-*n*T** complexes dissolved in distilled water. Steady state absorption-emission, resonance Raman and femtosecond transient absorption were collected under air-equilibrated conditions, whereas nanosecond transient absorption experiments were recorded both under aerated and deaerated conditions. Deaeration was achieved with five freeze-pump-thaw cycles under nitrogen. Samples for steady state emission were prepared in a 1 cm quartz cuvette at an OD of 0.05 at their respective long-wavelength absorption maxima. For resonance

Raman (excitation at 405 and 476 nm) and femtosecond transient absorption (excitation at 400 and 480 nm), samples were prepared at an OD of 0.2 at the respective pump wavelength in a 1 mm quartz cuvette. For nanosecond transient absorption experiments, samples were prepared to yield an OD of 0.25 at the pump wavelength (410 nm) in a 1 cm quartz cuvette.

Steady-state spectroscopy. UV-visible absorption spectra were recorded with a Jasco V-760 spectrophotometer. Steady-state emission measurements were carried out at the respective excitation maxima using a FLS980 spectrometer (Edinburgh Instruments). Resonance Raman (rR) spectra were recorded using 476 nm excitation from an argon ion laser (Coherent Innova 300C). The sample was placed in a rotating cell to avoid photo degradation.[30] The rR scattered light was collected at 90° from the incident light, focused on the entrance slit of an Acton SpectraPro 2750i spectrometer equipped with an 1800 line/mm grating yielding a resolution of 0.5 cm^{-1}, and detected with a liquid nitrogen cooled CCD camera from Princeton Instruments. rR spectra at 405 nm were recorded using a diode laser (Topmode-405-HP,Toptica) with the scattered light collected along the direction of incident light and detected by a spectrophotometer (Isoplane 160, Princeton Instruments) with a 1200 line/mm grating yielding a resolution of 3 cm^{-1}.Background correction was performed following established protocols based on peak detection by continuous wavelet transform (CWT), peak width estimation by signal-to-noise ratio (SNR) enhancing derivative calculation, and background fitting using penalized least squares with binary masks.[31]

Time-resolved spectroscopy. The setup for femtosecond transient absorption measurements has been described elsewhere.[32,33] The measurements were performed within a delay-time window of 2 ns upon excitation at 480 or 400 nm (temporal resolution 120 fs). A white light super continuum generated by focusing a residual of the fundamental laser pulses into a CaF_2 plate served as the probe light. The mutual polarization between the pump and the probe polarizations was set to magic angle.

Nanosecond transient absorption experiments were performed using a commercially available detection system from Pascher Instruments AB running on a 10 Hz NdYAG laser combined with an OPO yielding the 410 nm pump pulses. The system providing a temporal resolution of 10 ns was described elsewhere.[34]

RESULTS AND DISCUSSION

Steady-state absorption and emission spectroscopy. Figure 1b presents the absorption and emission spectra of the **Ru-ip-*n*T** series in comparison to the parent **Ru-ip-0T** complex lacking the thiophene rings. The prominent MLCT band is centered at around 450 nm for all complexes. In addition to the ^{1}MLCT absorption, a sharp ππ* absorption assigned to the dmb ligands and phenanthroline portion of the IP ligand is apparent below 300 nm.[35] The ^{1}MLCT absorption band exhibits a minor bathochromic shift as the number of thiophene rings increases, which is attributed to a slightly more delocalized LUMO afforded by additional thiophene rings. The more distinct feature associated with the presence of thiophene rings is the near-UV absorption band at 340 nm for **Ru-ip-1T** that shifts by 100 nm (6680 cm^{-1}) to 440 nm (for **Ru-ip-4T**). Similar systematic shifts of absorption features from 310 to 400 nm (7260 cm^{-1}) have been observed in the absorption spectra of the free bithiophene (2T), terthiophene (3T), and quaterthiophene (4T) in 1,4-dioxane.[36] Thus, the additional spectral features introduced by the presence of the thienyl groups are assigned to ligand-associated transitions on the oligothiophene chain. Theoretical calculations revealed that these ligand-associated states have a significant degree of charge transfer character, particularly in the case of **Ru-ip-3T** and **Ru-ip-4T**,[7,24] and are henceforth referred to as intraligand charge transfer (ILCT) states.

The steady-state emission spectra of the complexes are not affected by the length of the oligothiophene chain. The emission is centered at 630 nm for all of the complexes (Figure 1b) and closely resembles the emission spectrum of the archetype Ru(II) coordination complex

$[Ru(bpy)_3]^{2+}$.[35]This emission decays with a lifetime of 700 ns for **Ru-ip-0T** and **Ru-ip-1T**,[29] which is similar to the 1-μs lifetime of the ^{3}MLCT state that dominates the excited state dynamics of $[Ru(bpy)_3]^{2+}$ and other Ru(II) polypyridyl complexes. However, emission from **Ru-ip-2T** decays biexponentially with characteristic time constants of 0.7 and 14 μs, consistent with a model whereby the ^{3}MLCT state can also be populated from a nearby ^{3}IL state, resulting in the second emission lifetime. For **Ru-ip-3T** and **-4T** a single exponential decay with a lifetime of 0.7 μs is observed due to the fact that the lower-lying ^{3}ILCT states can no longer effectively populate the higher-lying ^{3}MLCT state.[29]

Resonance Raman spectroscopy. In order to detail the nature of the Franck-Condon state, resonance Raman (rR) spectra of the complexes in water were recorded upon excitation at 476 nm. Figure 1c depicts the rR spectra normalized to the band at 1320 cm^{-1}, which is associated with the Raman-active C-C stretching mode between the two pyridyl rings of the bpy-ligand.[37] Normalization of the spectra to the water band was not possible due to phosphorescence from the metal complex being superimposed on the rR spectra in the spectral range >2000 cm^{-1}.[34] All complexes show common rR bands at 1195, 1425, 1460, 1553 and 1624 cm^{-1}. These bands do not change with added thiophenes and are absent in $[Ru(bpy)_3]^{2+}$. Hence, these bands are assigned to vibrations arising from the IP ligand. Of these, the band at 1460 cm^{-1} can be assigned to the C=C stretching vibration from the phen portion of the IP ligand by comparison with literature.[38,39] The band at 1256 cm^{-1}, also absent in $[Ru(bpy)_3]^{2+}$, originates from a C_4-Me stretching mode of the dmb ligand.[30,40] This band is common irrespective of the number of thiophenes and highlights the presence of Raman-active dmb vibrations in all complexes.

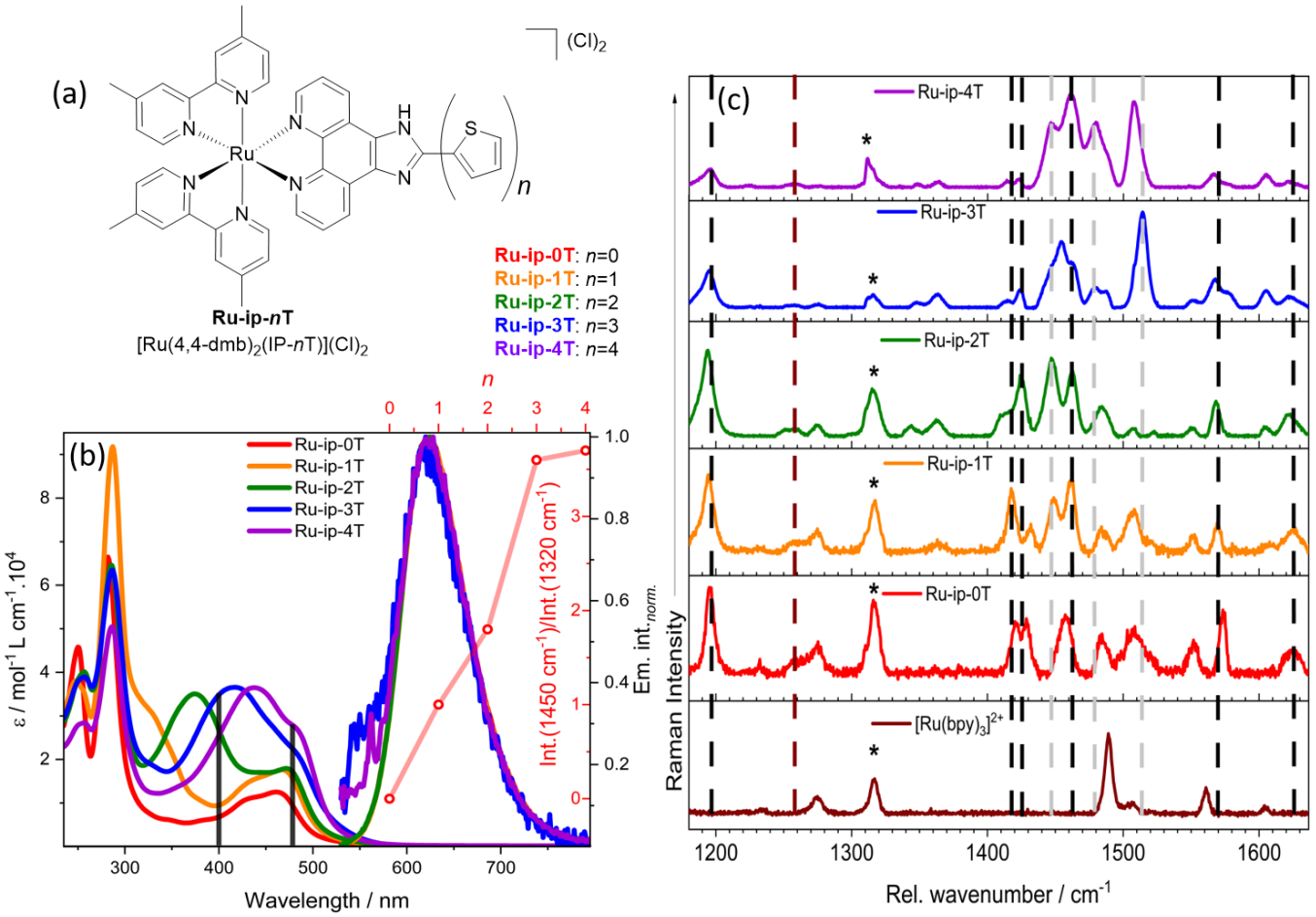

Figure 1. (a) Chemical structures of the complexes investigated. (b) Steady state UV-vis absorption and emission spectra of **Ru-ip-0T-4T** in water (emission spectra are normalized to the MLCT emission maximum at 640 nm). The UV-vis absorption and emission spectra were reported previously.[29] The ratio of the Resonance Raman band intensity at 1450 cm^{-1} (due to bpy) relative to that at 1320 cm^{-1} (due to the thienyl rings) are indicated by the red circles and show the increased contribution of the thienyl vibration with increasing *n* for **Ru-ip-0T-4T** with 476 nm excitation. (c) Resonance Raman spectra (normalized to the bpy band at 1320 cm^{-1}) of **Ru-ip-0T-4T** in water with 476 nm excitation. Resonance Raman bands associated with phen are marked by the vertical black dashed lines; thiophene-associated bands are marked by the grey dashed lines.

With 476-nm excitation, the ^{1}ILCT and ^{1}MLCT transitions overlap for **Ru-ip-3T** and **-4T** (Figure 1b). One of the most intense rR bands occurs near 1510 cm^{-1}, where oligothiophenes are known to show a Raman-active vibration due to C_α=C_β-H asymmetric stretching.[41,42] Raman-active vibrations associated with phen and dmb (as in **Ru-ip-0T** and $[Ru(bpy)_3]^{2+}$ respectively) also contribute in the same spectral range, and the relative contribution of the thiophene vibration can be estimated by the ratio of the intensity of the 1510 cm^{-1} band to that of the C-C bpy stretch at 1320 cm^{-1}. This ratio is less than 1 for

Ru-ip-0T to **-2T**. However, in **Ru-ip-3T** and **-4T** the ratio is >>1, indicating that oligothiophene vibrations contribute to the intense band at 1510 cm^{-1} and are prominent in these complexes. In line with this observation, a clear trend showing an increase in the contribution of thiophene vibration with increasing *n* can also be estimated from the ratio of the intensity of the thienyl band at 1450 cm^{-1} to the bpy band at 1320 cm^{-1} (Figure 1b). This distinct trend of increased peak intensity for the oligothienyl bands is also observed upon shifting the excitation wavelength from 476 to 405 nm (SI Figure S1). Thus, the rR data reflects the more preferential excitation of the oligothiophene chromophore with increasing *n*.

Time-resolved transient absorption spectroscopy. The photoinduced sub-ns relaxation kinetics within the **Ru-ip-*n*T** series starts with considering the data obtained for **Ru-ip-0T**[43] as the benchmark complex as well as **Ru-ip-1T** (Figure 2). The data were recorded upon photoexcitation at 480 nm. The femtosecond pump-probe data for both complexes is similar, marked by a ground-state bleach (GSB) between 375 and 500 nm, which is the spectral region where the ^{1}MLCT absorption dominates with no contribution from thienyl-based absorption. The GSB is flanked by excited-state absorption (ESA) below 375 nm due to ππ* absorption of the reduced coligands (and possibly the proximal portion of the ip ligand), and above 500 nm due to ligand-to-metal charge transfer (LMCT) from the reduced coligands to the oxidized Ru(III) metal center. The visible ESA is broad and featureless, characteristic of ^{3}MLCT states in the simpler $[Ru(bpy)_3]^{2+}$, $[Ru(phen)_3]^{2+}$, $[Ru(dmb)_3]^{2+}$ and $[Ru(bpy)_2(ip)]^{2+}$ complexes.[9,35,43] The temporal resolution of the experiment (120 fs) is insufficient to resolve the ultrafast intersystem crossing (ISC) from the initially excited ^{1}MLCT states to the triplet manifold.[35,44,45]

For both **Ru-ip-0T** and **Ru-ip-1T**, only very minor changes in the transient absorption spectra occur on the sub-ns timescale (after ISC to the triplet manifold). The intensity of the ESA band centered at 360 nm decreases slightly up to about 20 ps and also exhibits a small blue shift (300 cm^{-1}). Such features have been attributed to dissipation of excess vibrational energy from the initially hot ^{3}MLCT

states in $[Ru(bpy)_3]^{2+}$-derived complexes.[44] The resulting thermalized ^{3}MLCT state decays back to the ground state (Figure 2a, b) with characteristic time constants of 0.7 and 0.4 μs under deaerated and aerated conditions, respectively, for both **Ru-ip-0T** and **Ru-ip-1T**.[29,46]

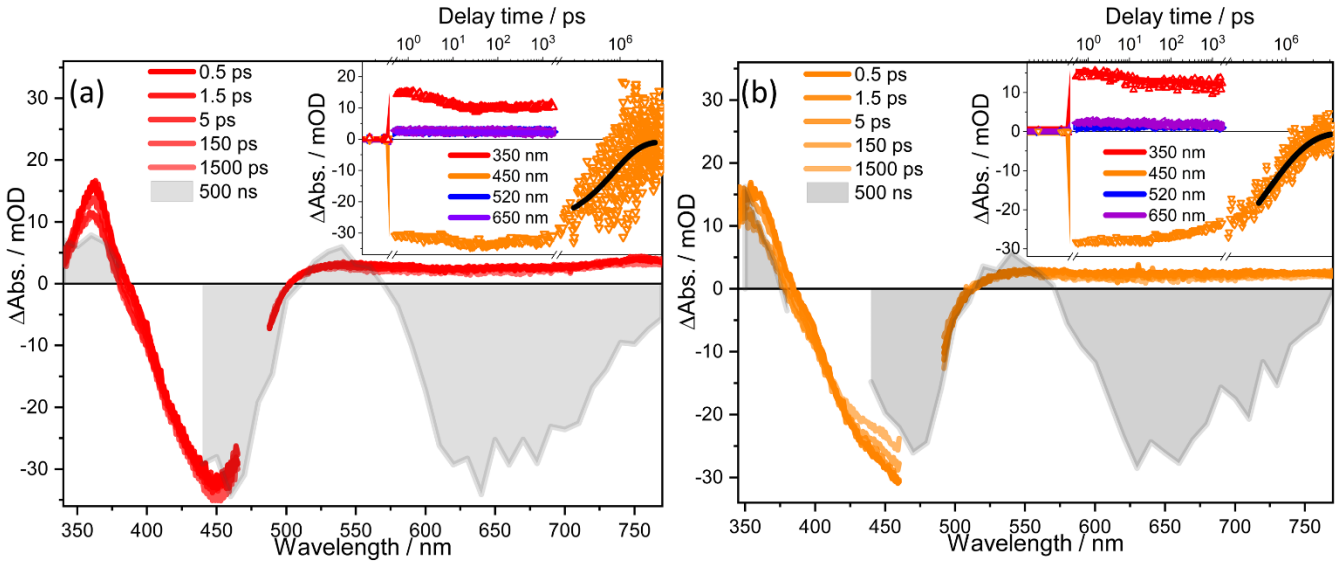

Figure 2. Femtosecond transient absorption spectra of **Ru-ip-0T** (a) and **Ru-ip-1T** (b) in water upon excitation at 480 nm at various delay times. The shaded spectra represent transient absorption spectra recorded at a delay time of 500 ns.[29] The strong negative differential absorption band at probe wavelengths longer than 570 nm is due to emission from the excited complex.[29] The insets show transient absorption kinetics at selected probe wavelengths. The ns transient absorption data has been reported previously[29] and is reproduced here to give a comprehensive summary of the overall excited-state decay.

The differential absorption spectrum of **Ru-ip-2T** recorded upon excitation of the ^{1}MLCT transitions at 480 nm resembles that of the photoexcited **Ru-ip-0T** and **Ru-ip-1T** at early times, with an initial bleach at the excitation wavelength concomitant with an ESA at 360 nm and at wavelengths >510 nm (Figure 3). Unlike what was observed for **Ru-ip-0T** and **Ru-ip-1T** where there was little change in the initially observed TA spectrum characteristic of the ^{3}MLCT state, the initially weak ESA band beyond 510 nm in the spectrum for **Ru-ip-2T** develops a pronounced maximum at 550 nm. The rise of the ESA maximum is partially superimposed on the negative ΔOD feature at 480 nm, causing a blue shift of the ΔOD zero crossing with increasing delay time.

Quantitative analysis of the data obtained for **Ru-ip-2T** employs a three-exponential global fit and yields characteristic time constants τ_1 = 1.3 ps, τ_2= 19 ps, and τ_3=1.1 ns, in addition to a much longer-lived component that does not decay over the timescale of these experiments.[29] The latter is assigned as T_1 and decays on the μs timescale according to previous ns emission and TA experiments.[29] The 1.3 ps component (τ_1) reflects positive ΔOD changes at 360 nm negative ΔOD changes at longer wavelengths. This is indicative of hot ^{3}MLCT → hot ^{3}ILCT energy transfer, following ultrafast ISC in the MLCT manifold.[44] The kinetic component characterized by the 19 ps component (τ_2) reflects the development of a pronounced ESA at 550 nm concomitant with the decay of the bleach between 400 and 500 nm and decay of the ESA at 360 nm. We associate these spectral changes to energy dissipation from the vibrationally hot ^{3}ILCT state to a thermally relaxed ^{3}ILCT state. We speculate that the formation of the thermally relaxed ^{3}ILCT state might be associated with a conformational change within the bithienyl unit. This assertion is consistent with computational analysis suggesting planarization of the lowest-lying triplet state.[7,8,24,45] The 1.1 ns time constant (τ_3) reflects the formation of an ESA in the range of the ground state absorption between about 420 and 520 nm. This increasing ESA on a 1.1 ns timescale causes the apparent GSB to diminish in this spectral region. These spectral changes are accompanied by a decay of the differential absorption signal at longer wavelengths. This slower process leads to an overall signal decay and is assigned to energy transfer from the relaxed ^{3}MLCT → relaxed ^{3}ILCT state.

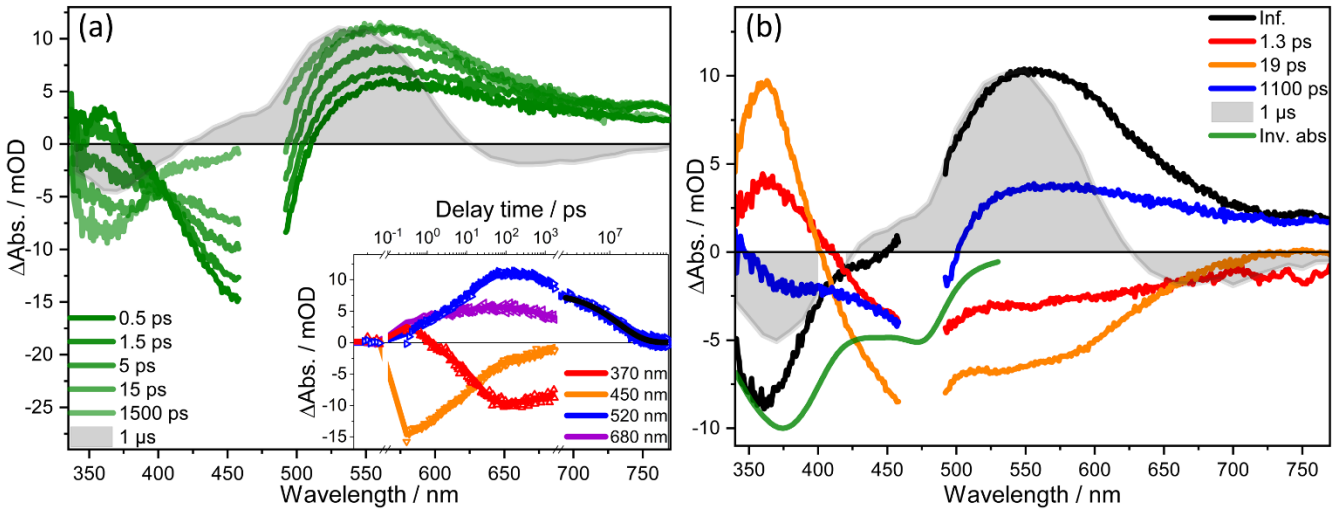

Figure 3. (a) Femtosecond TA spectra of **Ru-ip-2T** in water with 480 nm excitation at different delay times and a spectrum at 1 µs from nanosecond TA. The negative signal beyond 600 nm in the ns TA spectrum is due to phosphorescence from the complex. The inset shows kinetics at the respective wavelengths on the ps to µs time scale.[29] (b) DAS with the inverted absorption spectrum. The spectrum at 1 µs was determined by ns transient absorption spectroscopy, which has been reported previously.[26] The spectrum is included here to give a full account of excited state lifetimes.[29]

The decay of T_1 (i.e., the thermalized ^{3}ILCT state) has been monitored by ns-transient absorption and time-resolved emission spectroscopy.[29] In contrast to the complexes with fewer thiophene rings, **Ru-ip-2T** reveals a biphasic decay of the ^{3}MLCT emission with characteristic time constants of 0.6 and 11 µs.[29] The ns-transient absorption spectrum has the signature of the ^{3}ILCT state and decays with a characteristic time constant of 14 µs, which is very similar to the slow emission decay component.[29] The agreement between the longer decay time for the ^{3}MLCT state observed by ns-emission and the decay of the ^{3}ILCT state observed by ns-transient absorption suggests that the long-lived triplet excited state associated with the bithienyl chromophore acts as a reservoir to populate the emissive ^{3}MLCT states, leading to delayed emission.[7,24]

The photoinduced dynamics of **Ru-ip-3T** and **Ru-ip-4T** were similar (*vide infra*), but different from the complexes with fewer thiophene rings (Figure 4). Our discussion starts by considering **Ru-ip-3T**. Following excitation of a mixture of ^{1}MLCT and ^{1}ILCT transitions at 480 nm, a GSB occurs below

500 nm, while an ESA is apparent at longer wavelengths. The ESA rapidly evolves into a broad and intense band centered at 640 nm with a shoulder at around 550 nm. Concomitant with the spectral evolution of the ESA band, the negative differential absorption with a minimum at 410 nm also changes while the initially-observed strong negative feature at the pump wavelength disappears. The spectral changes are apparent up to about 70 ps, after which an overall decay of the signal is observed. The kinetic analysis requires a sum of three exponentials to fit the experimental data (Figure 4) yielding τ_1=2.5 ps, τ_2=43 ps, and τ_3=600 ps in addition to a much longer-lived component. The temporal evolution of the differential absorption band centered at 640 nm is associated with the three sub-ns kinetic components and will be key to account for the excited state relaxation in **Ru-ip-3T** and **-4T**.

The fast 2.5 ps component (τ_1) reflects the decay of the original bleach signal (characteristic for ground state → ^{1}MLCT/^{1}ILCT absorption) for **Ru-ip-3T** at around 480 nm, which is accompanied by a significant increase in the ESA centered at 640 nm. This spectral evolution reflects the build-up of the ^{3}ILCT state via energy transfer from the hot ^{3}MLCT state to the terthienyl-localized hot ^{3}ILCT state. ISC (^{1}MLCT → ^{3}MLCT) preceding the energy transfer in the triplet manifold is assumed to occur within the 120 fs temporal resolution of our experiment, as typically observed for Ru(II) polypyridyl complexes.[35,44,45] While direct ^{1}ILCT → ^{3}ILCT ISC could also form the ^{3}ILCT state, this pathway is assumed to be a minor channel, also occurring within the instrument response function, and is not captured in our experiments. The 43-ps kinetic component (τ_2) describes a further increase in the ESA maximum at 640 nm (the DAS exhibits a slightly negative ΔOD at 640 nm), which is characteristic for the ^{3}ILCT state, while a minor decrease of the positive ΔOD signal flanks the prominent ESA band (positive contributions to the DAS at ca. 550 nm and > 700 nm). The spectral changes associated with τ_2, reflected in the DAS, effectively increase the ESA band at the center (near 640 nm), while decreaseing the intensity of the ESA in the flanking regions around 550 and 700 nm. Hence, the process associated with τ_2 effectively sharpens the ESA absorption band (Figure 4b). These spectral changes are indicative

of relaxation within a given electronic state, which we ascribe to structural relaxation within the oligothenyl chain. DFT analysis on related Os(II) complexes supports a planarization of the triplet excited state with respect to the ground state, where the terminal thiophene ring is twisted out of plane by approximately 20°.[7,24]

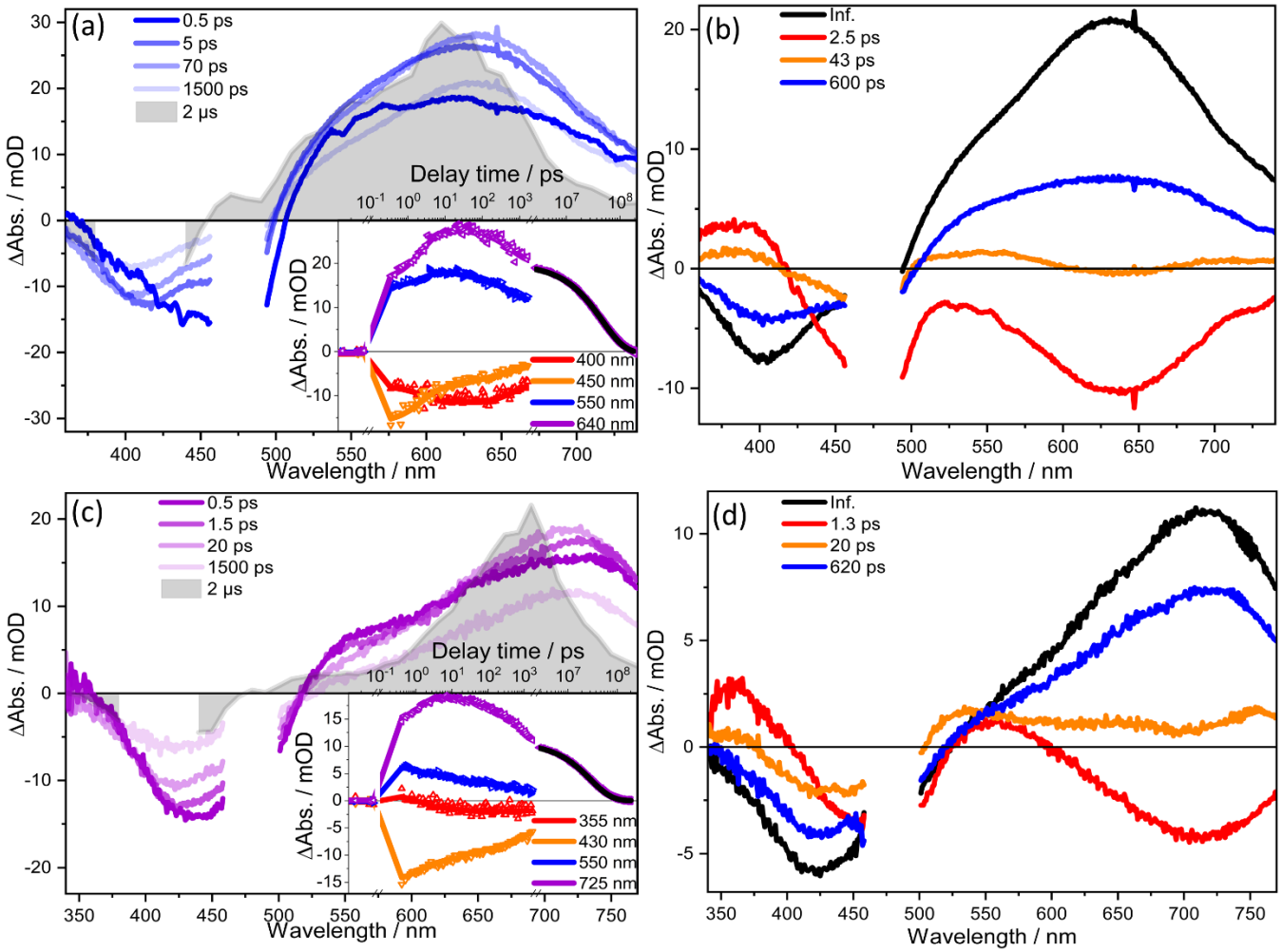

Figure 4. (a), (c) Femtosecond TA spectra of **Ru-ip-3T** and **Ru-ip-4T**, respectively, in water with 480 nm excitation at different delay times. The insets show the kinetics at the respective wavelengths on the ps and µs timescales for **Ru-ip-3T** and **Ru-ip-4T**, respectively. The previously published µs kinetic data is included to give a full account of the excited state lifetimes.[29] (b), (d) The DAS of **Ru-ip-3T** and **Ru-ip-4T**, respectively. The black curve (Inf.) refers to the infinite spectrum on the ultrafast timescale.

The 600 ps component (τ_3) reflects the further decay of a ^{3}ILCT-based state. In contrast to **Ru-ip-2T**, for which the slow ns-process associated with τ_3 reflects the rise of an ESA below 520 nm, the

process associated with τ_3 in **Ru-ip-3T** reflects a pronounced ground state recovery, indicating that in **Ru-ip-3T** τ_3 is associated with a relaxation channel back to the ground state. This ground-state recovery is associated with the loss of the broad ESA extending to the near-IR. We suggest that the conformational structures of the 3T and 4T units support two distinct cooled ^{3}ILCT states. In such a scenario, τ_3 reflects the deactivation channel of the ^{3}ILCT state with slightly higher energy relative to T_1. Depopulation of this higher lying ^{3}ILCT state occurs concurrent with ground-state recovery. Given the comparatively broad DAS for the 600 ps component (compared to the DAS of the μs component T_1), we propose that τ_3 stems from a conformational distribution of molecules in the ^{3}ILCT state that are distinct from that of the T_1 conformation.

The fs-TA data for **Ru-ip-4T** (Figure 4c, d) indicate a qualitatively similar excited-state evolution as **Ru-ip-3T**. Following excitation of a mixture of ^{1}MLCT and ^{1}ILCT states at 480 nm, the system relaxes to a long-lived state, which is characterized by a pronounced ESA at 720 nm. The kinetics of this process are accounted for by a three-exponential fit with the characteristic time constants τ_1=1.3 ps, τ_2=20 ps and τ_3=620 ps along with an additional long-lived component assigned as T_1. The DAS for τ_1 reveal a decay of the initial GSB associated with the MLCT/ILCT transitions between 410 and 525 nm that is simultaneous with the build-up of the ESA at 720 nm. Thus, we assign the 1.3 ps component (τ_1) to energy transfer from the hot ^{3}MLCT to a hot ^{3}ILCT state. Because the ^{3}ILCT absorption for **Ru-ip-4T** is bathochromically shifted compared to that for **Ru-ip-3T**, the peak having the strong negative contributions in the DAS (τ_1) of **Ru-ip-4T** is shifted to longer wavelengths compared to that for **Ru-ip-3T**. Population of the hot ^{3}ILCT state is followed by cooling within the ^{3}ILCT manifold to populate the structurally relaxed T_1 that decays with lifetime τ_{TA} as well as the structurally relaxed higher-lying ^{3}ILCT state that decays by τ_3 (*vide infra*). We assign τ_2 to this cooling process, which gives

rise to a blue shift of the ESA maxima as seen in the differential absorption spectra recorded at 1.5 and 20 ps (Figure 4c) that is indicative of a cooling process. The 620 ps component (τ_3) reflects a concerted decay of the GSB (below 525 nm) and the ESA (above 525 nm). The overall spectral shape is reminiscent of ^{3}ILCT absorption spectra for the long-lived T_1 state in the ns measurements, which was assigned as ^{3}ILCT.[26] In contrast to the DAS (τ_3) observed for **Ru-ip-3T**, that for **Ru-ip-4T** has a maximum beyond 700 nm. We ascribe this shift to the more elongated oligothienyl chain of **Ru-ip-4T**. As described for **Ru-ip-3T**, τ_3 may collectively encompass the sub-ns decay of a distribution of excited state conformers with slightly higher-lying ^{3}ILCT states compared to T_1. While the exact mechanisms that govern the slow decay of the triplet excited states are still under investigation, the data presented here taken together with the ns-transient absorption data (where the ^{3}ILCT-based T_1 lifetime is 29 μs) [29] reveal the presence of more than a single decaying ^{3}ILCT state.

Figure 5 summarizes the photophysical model for the **Ru-ip-*n*T** complexes as derived from the spectroscopic studies. Key to the model is the presence of an emissive manifold of ^{3}MLCT-based excited states and a dark manifold of ^{3}ILCT-based excited states. Depending on the length of the thiophene chain, the relative energies of the lowest-lying ^{3}MLCT and ^{3}ILCT states change, which in turn determines the photophysical properties. In **Ru-ip-2T** the ^{3}MLCT and the ^{3}ILCT states are nearly isoenergetic, enabling delayed ^{3}MLCT emission through population from the ^{3}ILCT state. The ^{3}ILCT states for **Ru-ip-3T** and **Ru-ip-4T**, however, are lower in energy than the ^{3}MLCT states so the majority of excited molecules decay through the ^{3}ILCT channel with a much smaller fraction deactivating via the ^{3}MLCT state. The final key piece to the model is that τ_3 from the femtosecond transient absorption measurements (600-630 ps) and the μs-lifetimes (29-48 μs) for **Ru-ip-3T** and **Ru-ip-4T** both have characteristic signatures of the ^{3}ILCT state but with drastically different decay rates. The faster τ_3 component is tentatively ascribed to a higher-lying ^{3}ILCT state from which a distribution of excited state

conformers decay, whereas the lowest-lying (T_1) state represents the decay of the planarized ^{3}ILCT state that has been described computationally.[7,24]

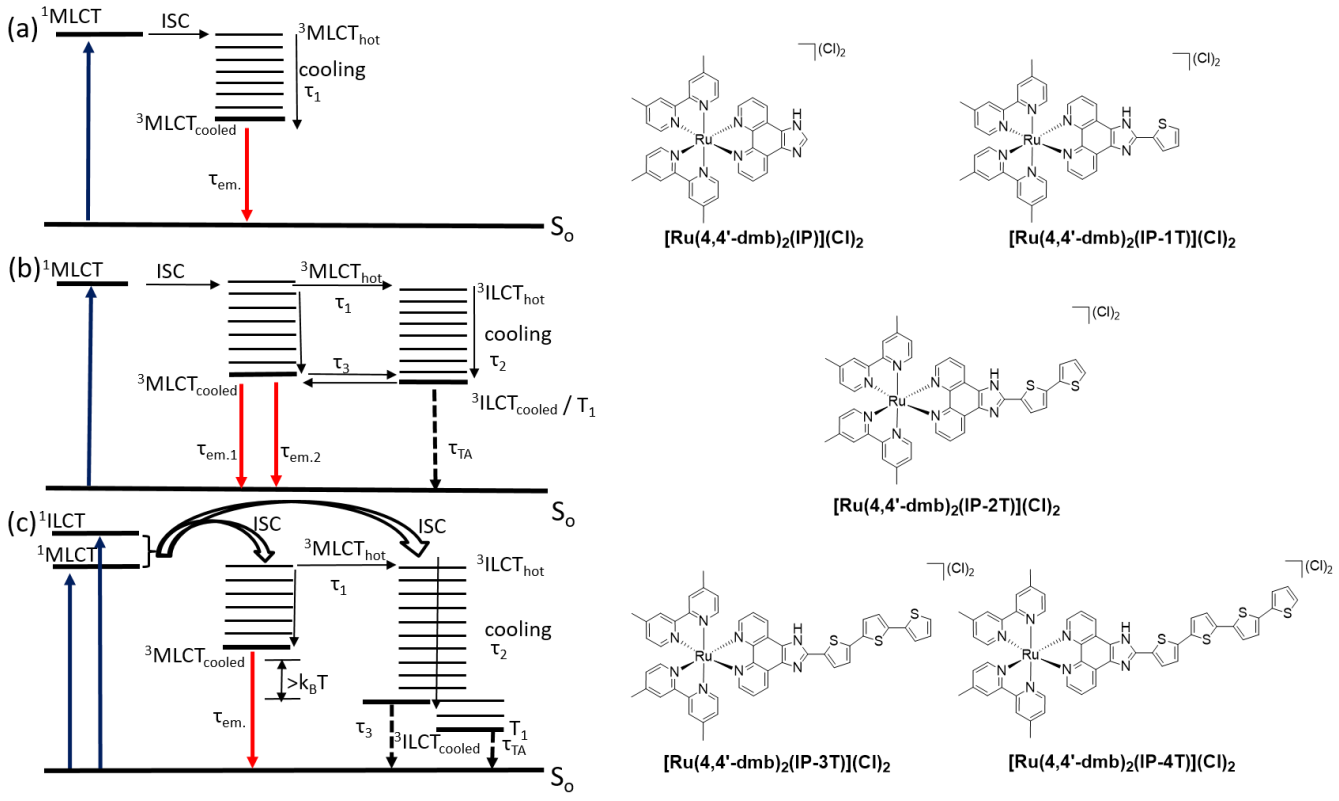

Figure 5. (a) Jablonski diagram for **Ru-ip-0T** and **Ru-ip-1T** where relaxation occurs via the emissive ^{3}MLCT state. (b) In **Ru-ip-2T** addition of a second thiophene ring to the chain leads to population of an ^{3}ILCT state which is nearly isoenergetic with the emissive ^{3}MLCT state. (c) In **Ru-ip-3T** and **Ru-ip-4T** the ^{3}ILCT state is highly stabilized and acts as a major relaxation pathway with only a minor fraction of molecules relaxing via the ^{3}MLCT state.

In order to evaluate the impact of the excitation wavelength and to further test the photophysical model (Figure 5), the **Ru-ip-*n*T** family was investigated using shorter-wavelength excitation at 400 nm. Excitation of **Ru-ip-0T** and **-1T** at 400 nm leads to differential absorption spectra and kinetics essentially identical to those observed upon excitation at 480 nm (Figure S2), where the TA spectra show only a minor blue shift of the ESA centered at 375 nm. The absence of an excitation wavelength-dependence reflects the fact that contributions from the oligothiophene-based ILCT states are absent for **Ru-ip-0T** and **-1T** and consequently excitation at both 480 and 400 nm populates only the ^{1}MLCT state.

The excess vibrational energy, which is delivered upon shorter wavelength excitation at 400 nm, is rapidly dissipated after excitation,[35,47] leading to sub-ns dynamics that are unaltered by changing the excitation wavelength.

Excitation of **Ru-ip-3T** (Figure 6) and **-4T** at 400 nm (Figure S4) yields an initial bleach signal at 480 nm in addition to the bleach at the excitation wavelength. These features point toward the simultaneous excitation of both ^{1}ILCT and ^{1}MLCT states (Figure 1). The initially broad ESA at wavelengths longer than 500 nm evolves into a well-defined peak at 660 nm (**Ru-ip-3T**) and 725 nm (**Ru-ip-4T**). As discussed above, this feature stems from the formation of a thermally relaxed ^{3}ILCT state, which decays on a μs timescale. The global fitting of the 400-nm data yields three characteristic time constants for both **Ru-ip-3T** and **-4T**. A sub-ps time constant, 0.6 ps for **Ru-ip-3T** and 0.7 ps for **Ru-ip-4T**, is associated with hot ^{3}MLCT state → hot ^{3}ILCT state energy transfer (following unresolved ^{1}MLCT → ^{3}MLCT ISC). Compared to 480-nm excitation, the hot ^{3}MLCT → hot ^{3}ILCT relaxation process for **Ru-ip-3T** with 400-nm excitation is four times faster. The reaction rate increases from $(2.5\ \text{ps})^{-1}$ to $(0.6\ \text{ps})^{-1}$ with shorter wavelength excitation, in agreement with excess energy deposited into the system. This further supports the role of vibronically hot excited states in promoting the ^{3}MLCT → ^{3}ILCT energy transfer. The subsequent processes in **Ru-ip-3T**, with time constants τ_2 = 4.4 ps and τ_3 = 920 ps, are assigned to the formation of the relaxed ^{3}ILCT state from the hot ^{3}ILCT state (τ_2) and deactivation of a fraction of molecules from the higher-lying ^{3}ILCT (τ_3) state under thermally relaxed conditions. While τ_3 is of the same order of magnitude for both excitation at 400 and 480 nm, τ_2 is shorter with shorter wavelength excitation. To account for this wavelength dependence of τ_2, we suggest different ground-state conformers associated with the terthiophene chain being excited at 400 versus 480 nm. These different sets of conformers may undergo different geometrical relaxation in their excited states, accounting for the observed pump-wavelength dependent time constant τ_2. A conceptually identical situation is observed for **Ru-ip-4T**, for which the time constant τ_2 decreases from 20 ps to 9.6 ps upon

shifting the excitation wavelength from 480 to 400 nm. The absence of a pump wavelength dependence for τ_3 may indicate the decay from one conformer.

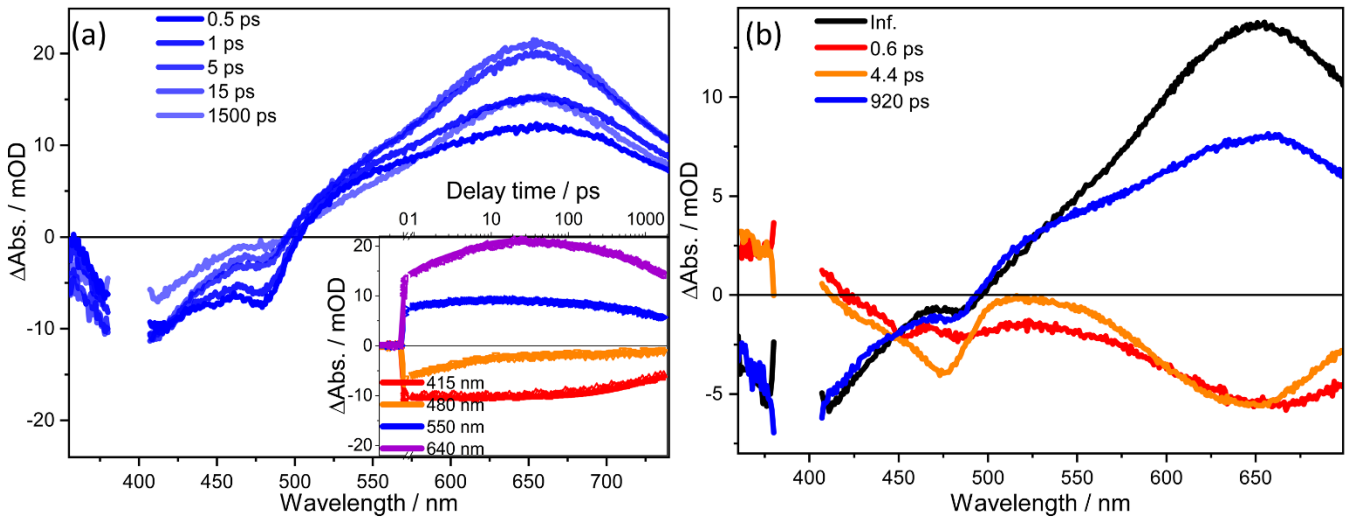

Figure 6 (a) Femtosecond TA spectra of **Ru-ip-3T** in water with 400-nm excitation at different delay times. The inset shows the kinetics at the respective wavelengths on the ps time scale. (b) DAS of **Ru-ip-3T.** The black curve (Inf.) refers to the infinite spectrum on the ultrafast timescale.

The systematic increase in the number of thiophene rings in the **Ru-ip-*n*T** family provides access to long-lived ^{3}ILCT states in **Ru-ip-2T**-**4T**. These stabilized states are formed due to the extended π system of the oligothiophene chromophore. Depending on the energy of these ^{3}ILCT states, they are isoenergetic and coupled to ^{3}MLCT states as in **Ru-ip-2T** or further stabilized and decoupled as in **Ru-ip-3T**-**4T**, resulting in a further increase in the lifetime of ^{3}ILCT states. This decoupled behavior of ^{3}MLCT and ^{3}ILCT states in **Ru-ip-3T**-**4T** is in part responsible for their potent photocytotoxicities as the ^{3}ILCT states are the longest-lived and as such should be most important for PDT effects.

CONCLUSIONS

We spectroscopically investigated the photophysical properties of a family of Ru(II) complexes, **Ru-ip-0T**-**4T**. One member (**Ru-ip-3T**) is currently in Phase 2 clinical trials for the treatment of human bladder

cancer. Our studies following the excited-state reaction pathway from the Franck-Condon point of absorption to the formation and decay of long-lived triplet states elucidate the role of the oligothiophene substituent in tuning the nature and the population dynamics of the long-lived triplet state. **Ru-ip-2T**-**4T**, with longer oligothiophene chains, show population of an ^{3}ILCT state in the picosecond regime formed predominantly via vibrational cooling of a hot ^{3}ILCT state. These hot ^{3}ILCT states in turn can be accessed directly from the hot ^{3}MLCT state. This is not the case in **Ru-ip-0T** and **-1T**, where ^{3}ILCT states are inaccessible and the excited state dynamics are dominated by ^{3}MLCT states. The accessibility of ^{3}ILCT states in **Ru-ip-2T**-**4T** was demonstrated in the μs regime for **Ru-ip-2T** where the ^{3}MLCT and ^{3}ILCT states are coupled, leading to delayed emission. These ^{3}ILCT states are further stabilized relative to the ^{3}MLCT state for **Ru-ip-3T** and **-4T**. This stabilization of the ^{3}ILCT state not only decouples it from ^{3}MLCT state but also prolongs its lifetime. The presence of these long-lived oligothiophene-based triplet states appears to be responsible for the very high phototoxicity of **Ru-ip-3T** and **-4T**.

ASSOCIATED CONTENTS

Supporting Information Resonance Raman spectra at 405 nm excitation of **Ru-ip-0**-**4T** in water, femtosecond transient absorption spectra and kinetics of **Ru-ip-0**-**1T** in water at 400 nm excitation, femtosecond transient absorption spectra, kinetics and DAS of **Ru-ip-2T** in water at 400 nm excitation and femtosecond transient absorption spectra, kinetics and DAS of **Ru-ip-4T** in water at 400 nm excitation, table with lifetimes of **Ru-ip-0**-**4T** from ps to μs time range, procedure for analysis of femtosecond transient absorption data.

AUTHOR INFORMATION

Corresponding authors

Sherri A. McFarland- The University of Texas at Arlington, Department of Chemistry and Biochemistry, Arlington, TX 76019, USA. E mail: sherri.mcfarland@uta.edu

Benjamin Dietzek- Leibniz-Institute of Photonic Technology Jena, Department Functional Interfaces, Albert-Einstein-Straße 9, 07745 Jena, Germany. E mail: benjamin.dietzek@leibniz-ipht.de

Friedrich-Schiller University Jena, Institute of Physical Chemistry, Helmholtzweg 4, 07743 Jena, Germany

Authors

Avinash Chettri- Leibniz-Institute of Photonic Technology Jena, Department Functional Interfaces, Albert-Einstein-Straße 9, 07745 Jena, Germany

Friedrich-Schiller University Jena, Institute of Physical Chemistry and Abbe Center of Photonics, Helmholtzweg 4, 07743 Jena, Germany; orcid.org/0000-0001-5500-5069

Kilian R.A. Schneider- Leibniz-Institute of Photonic Technology Jena, Department Functional Interfaces, Albert-Einstein-Straße 9, 07745 Jena, Germany

Friedrich-Schiller University Jena, Institute of Physical Chemistry, Helmholtzweg 4, 07743 Jena, Germany

Houston D. Cole- The University of Texas at Arlington, Department of Chemistry and Biochemistry, Arlington, TX 76019, USA

John A. Roque III- The University of Texas at Arlington, Department of Chemistry and Biochemistry, Arlington, TX 76019, USA

The University of North Carolina at Greensboro, Department of Chemistry and Biochemistry, Greensboro, NC 27402, USA

Colin G. Cameron- The University of Texas at Arlington, Department of Chemistry and Biochemistry, Arlington, TX 76019, USA

ACKNOWLEDGEMENTS

This work was supported by the German Science Foundation (grant No 395358570) and the Carl Zeiss Foundation via a PhD Fellowship to Kilian Rolf Anton Schneider.

S.A.M. has a potential research conflict of interest due to a financial interest with Theralase Technologies, Inc. and PhotoDynamic, Inc. A management plan has been created to preserve objectivity in research in accordance with UTA policy.

S.A.M. and C.G.C. thank the National Science Foundation (NSF) (award 2102459) and National Cancer Institute (NCI) of the National Institutes of Health (NIH) (award R01CA222227) for partial support. The content in this review is solely the responsibility of the authors and does not necessarily represent the official views of the National Institutes of Health.

REFERENCES

(1) McCaw, D. L.; Bryan, J. N. Photodynamic Therapy. *Cancer Manag. Small Anim. Pract.* **2009**, *90*, 163–166.

(2) Felsher, D. W. Cancer Revoked: Oncogenes as Therapeutic Targets. *Nat. Rev. Cancer* **2003**, *3*, 375–380.

(3) MacDonald, I. J.; Dougherty, T. J. Basic Principles of Photodynamic Therapy. *J. Porphyr. Phthalocyanines* **2001**, *5*, 105–129.

(4) Oleinick, N. L.; Evans, H. H. The Photobiology of Photodynamic Therapy: Cellular Targets and Mechanisms. *Radiat. Res.* **1998**, *150*, S146-S156.

(5) McKenzie, L. K.; Bryant, H. E.; Weinstein, J. A. Transition Metal Complexes as Photosensitisers in One- and Two-Photon Photodynamic Therapy. *Coord. Chem. Rev.* **2019**, *379*, 2–29.

(6) Castano, A. P.; Demidova, T. N.; Hamblin, M. R. Mechanisms in Photodynamic Therapy: Part One - Photosensitizers, Photochemistry and Cellular Localization. *Photodiagnosis Photodyn. Ther.* **2004**, *1*, 279–293.

(7) Roque, J. A.; Barrett, P. C.; Cole, H. D.; Lifshits, L. M.; Shi, G.; Monro, S.; Von Dohlen, D.; Kim, S.; Russo, N.; Deep, G., et al. Breaking the Barrier: An Osmium Photosensitizer with Unprecedented Hypoxic Phototoxicity for Real World Photodynamic Therapy. *Chem. Sci.* **2020**, *11*, 9784–9806.

(8) Schneider, K. R. A.; Chettri, A.; Cole, H.; Reglinski, K.; Brückmann, J.; Rogue, J.; Stumper, A.; Nauroozi, D.; Schmid, S.; Bäuerle, P., et al. Intracellular Photophysics of an Osmium Complex Bearing an Oligothiophene Extended Ligand. *Chem. A Eur. J.* **2020**, *26*, 14844–14851.

(9) Campagna, S.; Puntoriero, F.; Nastasi, F.; Bergamini, G.; Balzani, V. Photochemistry and Photophysics of Coordination Compounds: Ruthenium. *Top. Curr. Chem.* **2007**, *280*, 117–214.

(10) McClenaghan, N. D.; Leydet, Y.; Maubert, B.; Indelli, M. T.; Campagna, S. Excited-State

Equilibration: A Process Leading to Long-Lived Metal-to-Ligand Charge Transfer Luminescence in Supramolecular Systems. *Coord. Chem. Rev.* **2005**, *249*, 1336–1350.

(11) Reichardt, C.; Pinto, M.; Wächtler, M.; Stephenson, M.; Kupfer, S.; Sainuddin, T.; Guthmuller, J.; McFarland, S. A.; Dietzek, B. Photophysics of Ru(II) Dyads Derived from Pyrenyl-Substitued Imidazo[4,5-f][1,10]Phenanthroline Ligands. *J. Phys. Chem. A* **2015**, *119*, 3986–3994.

(12) Goze, C.; Kozlov, D. V.; Tyson, D. S.; Ziessel, R.; Castellano, F. N. Synthesis and Photophysics of Ruthenium(II) Complexes with Multiple Pyrenylethynylene Subunits. *New J. Chem.* **2003**, *27* , 1679–1683.

(13) Kozlov, D. V.; Tyson, D. S.; Goze, C.; Ziessel, R.; Castellano, F. N. Room Temperature Phosphorescence from Ruthenium(II) Complexes Bearing Conjugated Pyrenylethynylene Subunits. *Inorg. Chem.* **2004**, *43*, 6083–6092.

(14) Lincoln, R.; Kohler, L.; Monro, S.; Yin, H.; Stephenson, M.; Zong, R.; Chouai, A.; Dorsey, C.; Hennigar, R.; Thummel, R. P., et al. Exploitation of Long-Lived ^{3}IL Excited States for Metal-Organic Photodynamic Therapy: Verification in a Metastatic Melanoma Model. *J. Am. Chem. Soc.* **2013**, *135*, 17161–17175.

(15) Ford, W. E.; Rodgers, M. A. J. Reversible Triplet-Triplet Energy Transfer within a Covalently Linked Bichromophoric Molecule. *J. Phys. Chem.* **1992**, *96*, 2917–2920.

(16) Simon, J. A.; Curry, S. L.; Schmehl, R. H.; Schatz, T. R.; Piotrowiak, P.; Jin, X.; Thummel, R. P. Intramolecular Electronic Energy Transfer in Ruthenium(II) Diimine Donor/Pyrene Acceptor Complexes Linked by a Single C-C Bond. *J. Am. Chem. Soc.* **1997**, *119*, 11012–11022.

(17) Harriman, A.; Hissler, M.; Khatyr, A.; Ziessel, R. A Ruthenium(II) Tris(2,2'-bipyridine) Derivative Possessing a Triplet Lifetime of 42 µs. *Chem. Commun.* **1999**, *0*, 735–736.

(18) Shi, G.; Monro, S.; Hennigar, R.; Colpitts, J.; Fong, J.; Kasimova, K.; Yin, H.; DeCoste, R.; Spencer, C.; Chamberlain, L., et al. Ru(II) Dyads Derived from α-Oligothiophenes: A New Class of Potent and Versatile Photosensitizers for PDT. *Coord. Chem. Rev.* **2015**, *282–283*, 127–138.

(19) McFarland, S. A.; Mandel, A.; Dumoulin-White, R.; Gasser, G. Metal-Based Photosensitizers for Photodynamic Therapy: The Future of Multimodal Oncology? *Curr. Opin. Chem. Biol.* **2020**, *56*, 23–27.

(20) Monro, S.; Colón, K. L.; Yin, H.; Roque, J.; Konda, P.; Gujar, S.; Thummel, R. P.; Lilge, L.; Cameron, C. G.; McFarland, S. A. Transition Metal Complexes and Photodynamic Therapy from a Tumor-Centered Approach: Challenges, Opportunities, and Highlights from the Development of TLD1433. *Chem. Rev.* **2019**, *119*, 797–828.

(21) Heully, J. L.; Alary, F.; Boggio-Pasqua, M. Spin-Orbit Effects on the Photophysical Properties of $Ru(bpy)_3^{2+}$. *J. Chem. Phys.* **2009**, *131*, 1843080-1843089.

(22) Johansson, E. M. J.; Odelius, M.; Plogmaker, S.; Gorgoi, M.; Svensson, S.; Siegbahn, H.; Rensmo, H. Spin-Orbit Coupling and Metala-Ligand Interactions in Fe(II), Ru(II), and Os(II) Complexes. *J. Phys. Chem. C* **2010**, *114*, 10314–10322.

(23) Hall, R. D.; Chignell, C. F. Steady-State Near-Infrared Detection of Singlet Molecular Oxygen: A Stern-Volmer Quenching Experiment With Sodium Azide. *Photochem. Photobiol.* **1987**, *45* (4), 459–464.

(24) Roque, J. A.; Barrett, P. C.; Cole, H. D.; Lifshits, L. M.; Bradner, E.; Shi, G.; von Dohlen, D.; Kim, S.; Russo, N.; Deep, G., et al. Os(II) Oligothienyl Complexes as a Hypoxia-Active Photosensitizer Class for Photodynamic Therapy. *Inorg. Chem.* **2020**, *59*, 16341–16360.

(25) Ghosh, G.; Colón, K. L.; Fuller, A.; Sainuddin, T.; Bradner, E.; McCain, J.; Monro, S. M. A.; Yin,

H.; Hetu, M. W.; Cameron, C. G., et al. Cyclometalated Ruthenium(II) Complexes Derived from α-Oligothiophenes as Highly Selective Cytotoxic or Photocytotoxic Agents. *Inorg. Chem.* **2018**, *57*, 7694–7712.

(26) Monro, S.; Cameron, C. G.; Zhu, X.; Colón, K. L.; Yin, H.; Sainuddin, T.; Hetu, M.; Pinto, M.; Fuller, A.; Bennett, L., et al. Synthesis, Characterization and Photobiological Studies of Ru(II) Dyads Derived from α-Oligothiophene Derivatives of 1,10-Phenanthroline. *Photochem. Photobiol.* **2019**, *95*, 267–279.

(27) Sainuddin, T.; Pinto, M.; Yin, H.; Hetu, M.; Colpitts, J.; McFarland, S. A. Strained Ruthenium Metal-Organic Dyads as Photocisplatin Agents with Dual Action. *J. Inorg. Biochem.* **2016**, *158*, 45–54.

(28) Majewski, M. B.; Tacconi, N. R. D.; MacDonnell, F. M.; Wolf, M. O. Ligand-Triplet-Fueled Long-Lived Charge Separation in Ruthenium(II) Complexes with Bithienyl-Functionalized Ligands. *Inorg. Chem.* **2011**, *50*, 9939–9941.

(29) Chettri, A.; Roque, J. A.; Schneider, K. R. A.; Cole, H. D.; Cameron, C. G.; McFarland, S. A.; Dietzek, B. It Takes Three to Tango: The Length of the Oligothiophene Chain Determines the Nature of the Long-Lived Excited State and the Resulting Photocytotoxicity of a Ruthenium(II) Photodrug. *ChemPhotoChem* **2021**, *5*, 1–6.

(30) Kiefer, W. Raman Difference Spectroscopy with the Rotating Cell. *Appl. Spectrosc.* **1973**, *27*, 253–257.

(31) Zhang, Z. M.; Chen, S.; Liang, Y. Z.; Liu, Z. X.; Zhang, Q. M.; Ding, L. X.; Ye, F.; Zhou, H. An Intelligent Background-Correction Algorithm for Highly Fluorescent Samples in Raman Spectroscopy. *J. Raman Spectrosc.* **2010**, *41*, 659–669.

(32) Karnahl, M.; Kuhnt, C.; Ma, F.; Yartsev, A.; Schmitt, M.; Dietzek, B.; Rau, S.; Popp, J. Tuning of Photocatalytic Hydrogen Production and Photoinduced Intramolecular Electron Transfer Rates by Regioselective Bridging Ligand Substitution. *ChemPhysChem* **2011**, *12*, 2101–2109.

(33) Siebert, R.; Akimov, D.; Schmitt, M.; Winter, A.; Schubert, U. S.; Dietzek, B.; Popp, J. Spectroscopic Investigation of the Ultrafast Photoinduced Dynamics in π-Conjugated Terpyridines. *ChemPhysChem* **2009**, *10*, 910–919.

(34) Stephenson, M.; Reichardt, C.; Pinto, M.; Wächtler, M.; Sainuddin, T.; Shi, G.; Yin, H.; Monro, S.; Sampson, E.; Dietzek, B., et al. Ru (II) Dyads Derived from 2 - (1-Pyrenyl) - 1 H -imidazo[4,5-*f*][1,10]phenanthroline: Versatile Photosensitizers for Photodynamic Applications. *J. Phys. Chem. A* **2014**, *118*, 10507–10521.

(35) Damrauer, N. H.; Cerullo, G.; Yeh, A.; Boussie, T. R.; Shank, C. V; McCusker, J. K. Femtosecond Dynamics of Excited-State Evolution in $[Ru(bpy)_3]^{2+}$. *Science* **1997**, *275*, 54–57.

(36) Grebner, D.; Helbig, M.; Rentsch, S. Size-Dependent Properties of Oligothiophenes by Picosecond Time-Resolved Spectroscopy. *J. Phys. Chem.* **1995**, *99*, 16991–16998.

(37) Baiardi, A.; Latouche, C.; Bloino, J.; Barone, V. Accurate yet Feasible Computations of Resonance Raman Spectra for Metal Complexes in Solution: $[Ru(bpy)_3]^{2+}$ as a Case Study. *Dalt. Trans.* **2014**, *43*, 17610–17614.

(38) Coates, C. G.; Callaghan, P. L.; McGarvey, J. J.; Kelly, J. M.; Kruger, P. E.; Higgins, M. E. Transient Resonance Raman Investigation of Excited States of $[Ru(phen)_2dppz]^{2+}$ and Deuterated Analogues in Aqueous and Non-Aqueous Environments. *J. Raman Spectrosc.* **2000**, *31*, 283–288.

(39) Chen, W.; Turro, C.; Friedman, L. A.; Barton, J. K.; Turro, N. J. Resonance Raman Investigation of $Ru(phen)_2(dppz)^{2+}$ and Related Complexes in Water and in the Presence of DNA. *J. Phys.*

Chem. B **1997**, *101*, 6995–7000.

(40) McClanahan, S. F.; Dallinger, R. F.; Holler, F. J.; Kincaid, J. R. Mixed-Ligand Poly(Pyridine) Complexes of Ruthenium(II). Resonance Raman Spectroscopic Evidence for Selective Population of Ligand-Localized ^{3}MLCT Excited States. *J. Am. Chem. Soc.* **1985**, *107*, 4853–4860.

(41) Castro, C. M.; Delgado, M. C. R.; Hernández, V.; Hotta, S.; Casado, J.; López Navarrete, J. T. Efficiency of the π Conjugation in a Novel Family of α,A′-Bisphenyl End-Capped Oligothiophenes by Means of Raman Spectroscopy. *J. Chem. Phys.* **2002**, *116*, 10419–10427.

(42) Louarn, G.; Buisson, J. P.; Lefrant, S.; Fichou, D. Vibrational Studies of a Series of α-Oligothiophenes as Model Systems of Polythiophene. *J. Phys. Chem.* **1995**, *99*, 11399–11404.

(43) Peuntinger, K.; Pilz, T. D.; Staehle, R.; Schaub, M.; Kaufhold, S.; Petermann, L.; Wunderlin, M.; Görls, H.; Heinemann, F. W.; Li, J., et al. Carbene Based Photochemical Molecular Assemblies for Solar Driven Hydrogen Generation. *Dalt. Trans.* **2014**, *43*, 13683–13695.

(44) Cannizzo, A.; Van Mourik, F.; Gawelda, W.; Zgrablic, G.; Bressler, C.; Chergui, M. Broadband Femtosecond Fluorescence Spectroscopy of $[Ru(bpy)_3]^{2+}$. *Angew. Chemie - Int. Ed.* **2006**, *45*, 3174–3176.

(45) Bhasikuttan, A. C.; Suzuki, M.; Nakashima, S.; Okada, T. Ultrafast Fluorescence Detection in Tris(2,2′-bipyridine)ruthenium(II) Complex in Solution: Relaxation Dynamics Involving Higher Excited States. *J. Am. Chem. Soc.* **2002**, *124*, 8398–8405.

(46) Fetterolf, M. L.; Offen, H. W. Luminescence Lifetimes of Ruthenium(II) Polypyridyls in H_2O and D_2O at High Pressures. *J. Phys. Chem.* **1986**, *90*, 1828–1830.

(47) Damrauer, N. H.; McCusker, J. K. Ultrafast Dynamics in the Metal-to-Ligand Charge Transfer

Excited-State Evolution of [Ru(4,4′-diphenyl-2,2′-bipyridine)$_3$]$^{2+}$. *J. Phys. Chem. A* **1999**, *103*, 8440–8446.

TOC IMAGE

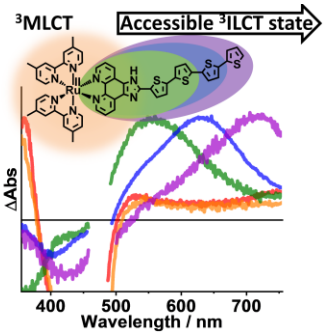
^{3}MLCT
Accessible ^{3}ILCT state
ΔAbs
400
500
600
700
Wavelength / nm